Improved measurement of absolute branching fraction of Ds(+) -> tau(+) v(tau)

P. U. E. Onyisi, J. L. Rosner, J. P. Alexander, D. G. Cassel, J. E. Duboscq, R. Ehrlich, L. Fields, R. S. Galik, L. Gibbons, R. Gray, S. W. Gray, D. L. Hartill, B. K. Heltsley, D. Hertz, J. M. Hunt, J. Kandaswamy, D. L. Kreinick, V. E. Kuznetsov, J. Ledoux, H. Mahlke-Kruger, D. Mohapatra, J. R. Patterson, D. Peterson, D. Riley, A. Ryd, A. J. Sadoff, X. Shi, S. Stroiney, W. M. Sun, T. Wilksen, S. B. Athar, J. Yelton, P. Rubin, N. Lowrey, S. Mehrabyan, M. Selen, J. Wiss, R. E. Mitchell, M. R. Shepherd, D. Besson, T. K. Pedlar, D. Cronin-Hennessy, K. Y. Gao, J. Hietala, Y. Kubota, T. Klein, R. Poling, A. W. Scott, P. Zweber, S. Dobbs, Z. Metreveli, K. K. Seth, B. J. Y. Tan, A. Tomaradze, J. Libby, L. Martin, A. Powell, G. Wilkinson, H. Mendez, J. Y. Ge, D. H. Miller, V. Pavlunin, B. Sanghi, I. P. J. Shipsey, B. Xin, G. S. Adams, D. Hu, B. Moziak, J. Napolitano, K. M. Ecklund, Q. He, J. Insler, H. Muramatsu, C. S. Park, E. H. Thorndike, F. Yang, M. Artuso, S. Blusk, S. Khalil, J. Li, R. Mountain, K. Randrianarivony, N. Sultana, T. Skwarnicki, S. Stone, J. C. Wang, L. M. Zhang, G. Bonvicini, D. Cinabro, M. Dubrovin, A. Lincoln, M. J. Smith, P. Naik, J. Rademacker, D. M. Asner, K. W. Edwards, J. Reed, A. N. Robichaud, G. Tatishvili, E. J. White, R. A. Briere, and H. Vogel

Improved measurement of absolute branching fraction of $D_s^+ \to \tau^+ \nu_\tau$

P. U. E. Onyisi,[1] J. L. Rosner,[1] J. P. Alexander,[2] D. G. Cassel,[2] J. E. Duboscq,[2,*] R. Ehrlich,[2] L. Fields,[2] R. S. Galik,[2] L. Gibbons,[2] R. Gray,[2] S. W. Gray,[2] D. L. Hartill,[2] B. K. Heltsley,[2] D. Hertz,[2] J. M. Hunt,[2] J. Kandaswamy,[2] D. L. Kreinick,[2] V. E. Kuznetsov,[2] J. Ledoux,[2] H. Mahlke-Krüger,[2] D. Mohapatra,[2] J. R. Patterson,[2] D. Peterson,[2] D. Riley,[2] A. Ryd,[2] A. J. Sadoff,[2] X. Shi,[2] S. Stroiney,[2] W. M. Sun,[2] T. Wilksen,[2] S. B. Athar,[3] J. Yelton,[3] P. Rubin,[4] N. Lowrey,[5] S. Mehrabyan,[5] M. Selen,[5] J. Wiss,[5] R. E. Mitchell,[6] M. R. Shepherd,[6] D. Besson,[7] T. K. Pedlar,[8] D. Cronin-Hennessy,[9] K. Y. Gao,[9] J. Hietala,[9] Y. Kubota,[9] T. Klein,[9] R. Poling,[9] A. W. Scott,[9] P. Zweber,[9] S. Dobbs,[10] Z. Metreveli,[10] K. K. Seth,[10] B. J. Y. Tan,[10] A. Tomaradze,[10] J. Libby,[11] L. Martin,[11] A. Powell,[11] G. Wilkinson,[11] H. Mendez,[12] J. Y. Ge,[13] D. H. Miller,[13] V. Pavlunin,[13] B. Sanghi,[13] I. P. J. Shipsey,[13] B. Xin,[13] G. S. Adams,[14] D. Hu,[14] B. Moziak,[14] J. Napolitano,[14] K. M. Ecklund,[15] Q. He,[16] J. Insler,[16] H. Muramatsu,[16] C. S. Park,[16] E. H. Thorndike,[16] F. Yang,[16] M. Artuso,[17] S. Blusk,[17] S. Khalil,[17] J. Li,[17] R. Mountain,[17] K. Randrianarivony,[17] N. Sultana,[17] T. Skwarnicki,[17] S. Stone,[17] J. C. Wang,[17] L. M. Zhang,[17] G. Bonvicini,[18] D. Cinabro,[18] M. Dubrovin,[18] A. Lincoln,[18] M. J. Smith,[18] P. Naik,[19] J. Rademacker,[19] D. M. Asner,[20] K. W. Edwards,[20] J. Reed,[20] A. N. Robichaud,[20] G. Tatishvili,[20] E. J. White,[20] R. A. Briere,[21] and H. Vogel[21]

(CLEO Collaboration)

[1]*Enrico Fermi Institute, University of Chicago, Chicago, Illinois 60637, USA*
[2]*Cornell University, Ithaca, New York 14853, USA*
[3]*University of Florida, Gainesville, Florida 32611, USA*
[4]*George Mason University, Fairfax, Virginia 22030, USA*
[5]*University of Illinois, Urbana-Champaign, Illinois 61801, USA*
[6]*Indiana University, Bloomington, Indiana 47405, USA*
[7]*University of Kansas, Lawrence, Kansas 66045, USA*
[8]*Luther College, Decorah, Iowa 52101, USA*
[9]*University of Minnesota, Minneapolis, Minnesota 55455, USA*
[10]*Northwestern University, Evanston, Illinois 60208, USA*
[11]*University of Oxford, Oxford OX1 3RH, United Kingdom*
[12]*University of Puerto Rico, Mayaguez, Puerto Rico 00681*
[13]*Purdue University, West Lafayette, Indiana 47907, USA*
[14]*Rensselaer Polytechnic Institute, Troy, New York 12180, USA*
[15]*Rice University; Houston, Texas 77005, USA*
[16]*University of Rochester, Rochester, New York 14627, USA*
[17]*Syracuse University, Syracuse, New York 13244, USA*
[18]*Wayne State University, Detroit, Michigan 48202, USA*
[19]*University of Bristol, Bristol BS8 1TL, United Kingdom*
[20]*Carleton University, Ottawa, Ontario, Canada K1S 5B6*
[21]*Carnegie Mellon University, Pittsburgh, Pennsylvania 15213, USA*
(Received 12 January 2009; published 11 March 2009)

We have studied the leptonic decay $D_s^+ \to \tau^+ \nu_\tau$, via the decay channel $\tau^+ \to e^+ \nu_e \bar{\nu}_\tau$, using a sample of tagged D_s^+ decays collected near the $D_s^{*\pm} D_s^{\mp}$ peak production energy in e^+e^- collisions with the CLEO-c detector. We obtain $\mathcal{B}(D_s^+ \to \tau^+ \nu_\tau) = (5.30 \pm 0.47 \pm 0.22)\%$ and determine the decay constant $f_{D_s} = (252.5 \pm 11.1 \pm 5.2)$ MeV, where the first uncertainties are statistical and the second are systematic.

DOI: 10.1103/PhysRevD.79.052002 PACS numbers: 13.20.Fc

I. INTRODUCTION

The leptonic decays of a charged pseudoscalar meson P^+ are processes of the type $P^+ \to \ell^+ \nu_\ell$, where $\ell = e$, μ, or τ. Because no strong interactions are present in the leptonic final state $\ell^+ \nu_\ell$, such decays provide a clean way to probe the complex, strong interactions that bind the quark and antiquark within the initial-state meson. In these decays, strong interaction effects can be parametrized by a single quantity, f_P, the pseudoscalar meson decay constant. The leptonic decay rate can be measured by experiment, and the decay constant can be determined

*Deceased.

by the equation (ignoring radiative corrections)

$$\Gamma(P_{Q\bar{q}} \to \ell^+ \nu_\ell) = \frac{G_F^2 |V_{Qq}|^2 f_P^2}{8\pi} m_P m_\ell^2 \left(1 - \frac{m_\ell^2}{m_P^2}\right)^2, \quad (1)$$

where G_F is the Fermi coupling constant, V_{Qq} is the Cabibbo-Kobayashi-Maskawa (CKM) matrix [1,2] element, m_P is the mass of the meson, and m_ℓ is the mass of the charged lepton. The quantity f_P describes the amplitude for the Q and $\bar{q}$-quarks within the P to have zero separation, a condition necessary for them to annihilate into the virtual W^+ boson that produces the $\ell^+ \nu_\ell$ pair.

The experimental determination of decay constants is one of the most important tests of calculations involving nonperturbative QCD. Such calculations have been performed using various models [3] or using lattice QCD (LQCD). The latter is now generally considered to be the most reliable way to calculate the quantity.

Knowledge of decay constants is important for describing several key processes, such as $B - \bar{B}$ mixing, which depends on f_B, a quantity that is also predicted by LQCD calculations. Experimental determination [4,5] of f_B with the leptonic decay of a B^+ meson is, however, very limited as the rate is highly suppressed due to the smallness of the magnitude of the relevant CKM matrix element V_{ub}. The charm mesons, D^+ and D_s^+, are better instruments to study the leptonic decays of heavy mesons since these decays are either less CKM suppressed or favored, i.e., $\Gamma(D^+ \to \ell^+ \nu_\ell) \propto |V_{cd}|^2 \approx (0.23)^2$ and $\Gamma(D_s^+ \to \ell^+ \nu_\ell) \propto |V_{cs}|^2 \approx (0.97)^2$ are much larger than $\Gamma(B^+ \to \ell^+ \nu_\ell) \propto |V_{ub}|^2 \approx (0.004)^2$. Thus, the decay constants f_D and f_{D_s} determined from charm meson decays can be used to test and validate the necessary LQCD calculations applicable to the B-meson sector.

Among the leptonic decays in the charm-quark sector, $D_s^+ \to \ell^+ \nu_\ell$ decays are more accessible since they are CKM favored. Furthermore, the large mass of the τ lepton removes the helicity suppression that is present in the decays to lighter leptons. The existence of multiple neutrinos in the final state, however, makes measurement of this decay challenging.

Physics beyond the standard model (SM) might also affect leptonic decays of charmed mesons. Depending on the non-SM features, the ratio of $\Gamma(D^+ \to \ell^+ \nu_\ell)/\Gamma(D_s^+ \to \ell^+ \nu_\ell)$ could be affected [6], as could the ratio [7,8] $\Gamma(D_s^+ \to \tau^+ \nu_\tau)/\Gamma(D_s^+ \to \mu^+ \nu_\mu)$. Any of the individual widths might be increased or decreased. There is an indication of a discrepancy between the experimental determinations [3] of f_{D_s} and the most recent precision LQCD calculation [9]. This disagreement is particularly puzzling since the CLEO-c determination [10] of f_D agrees well with the LQCD calculation [9] of that quantity. Some [11] conjecture that this discrepancy may be explained by a charged Higgs boson or a leptoquark.

In this article, we report an improved measurement of the absolute branching fraction of the leptonic decay $D_s^+ \to \tau^+ \nu_\tau$ (charge-conjugate modes are implied), with $\tau^+ \to e^+ \nu_e \bar{\nu}_\tau$, from which we determine the decay constant f_{D_s}.

II. DATA AND THE CLEO-C DETECTOR

We use a data sample of $e^+ e^- \to D_s^{*\pm} D_s^{\mp}$ events provided by the Cornell Electron Storage Ring (CESR) and collected by the CLEO-c detector at the center-of-mass (CM) energy 4170 MeV, near $D_s^{*\pm} D_s^{\mp}$ peak production [12]. The data sample consists of an integrated luminosity of 602 pb^{-1} containing 5.5×10^5 $D_s^{*\pm} D_s^{\mp}$ pairs. We have previously reported [13,14] measurements of $D_s^+ \to \mu^+ \nu_\mu$ and $D_s^+ \to \tau^+ \nu_\tau$ with a subsample of these data. A companion article [15] reports measurements of f_{D_s} from $D_s^+ \to \mu^+ \nu_\mu$ and $D_s^+ \to \tau^+ \nu_\tau$, with $\tau^+ \to \pi^+ \bar{\nu}_\tau$, using essentially the same data sample as the one used in this measurement.

The CLEO-c detector [16–19] is a general-purpose solenoidal detector with four concentric components utilized in this measurement: a small-radius six-layer stereo wire drift chamber, a 47-layer main drift chamber, a Ring-Imaging Cherenkov (RICH) detector, and an electromagnetic calorimeter consisting of 7800 CsI(Tl) crystals. The two drift chambers operate in a 1.0 T magnetic field and provide charged particle tracking in a solid angle of 93% of 4π. The chambers achieve a momentum resolution of $\sim$0.6% at $p = 1$ GeV/c. The main drift chamber also provides specific-ionization (dE/dx) measurements that discriminate between charged pions and kaons. The RICH detector covers approximately 80% of 4π and provides additional separation of pions and kaons at high momentum. The photon energy resolution of the calorimeter is 2.2% at $E_\gamma = 1$ GeV and 5% at 100 MeV. Electron identification is based on a likelihood variable that combines the information from the RICH detector, dE/dx, and the ratio of electromagnetic shower energy to track momentum (E/p).

We use a GEANT-based [20] Monte Carlo (MC) simulation program to study efficiency of signal-event selection and background processes. Physics events are generated by EVTGEN [21], tuned with much improved knowledge of charm decays [22,23], and final-state radiation (FSR) is modeled by the PHOTOS [24] program. The modeling of initial-state radiation (ISR) is based on cross sections for $D_s^{*\pm} D_s^{\mp}$ production at lower energies obtained from the CLEO-c energy scan [12] near the CM energy where we collect the sample.

III. ANALYSIS METHOD

The presence of two $D_s^{\mp}$ mesons in a $D_s^{*\pm} D_s^{\mp}$ event allows us to define a single-tag (ST) sample in which a $D_s^{\mp}$ is reconstructed in a hadronic decay mode and a further double-tagged (DT) subsample in which an additional $e^{\pm}$ is required as a signature of $\tau^{\pm}$ decay, the $e^{\pm}$ being the

daughter of the $\tau^{\pm}$. The D_s^- reconstructed in the ST sample can be either primary or secondary from $D_s^{*-} \to D_s^- \gamma$ (or $D_s^{*-} \to \pi^0 D_s^-$). The ST yield can be expressed as

$$n_{\rm ST} = 2N\mathcal{B}_{\rm ST}\epsilon_{\rm ST}, \tag{2}$$

where N is the produced number of $D_s^{*\pm}D_s^{\mp}$ pairs, $\mathcal{B}_{\rm ST}$ is the branching fraction of hadronic modes used in the ST sample, and $\epsilon_{\rm ST}$ is the ST efficiency. The $n_{\rm ST}$ counts the candidates, not events, and the factor of 2 comes from the sum of D_s^+ and D_s^- tags.

Our double-tag (DT) sample is formed from events with only a single charged track, identified as an e^+, in addition to a ST. The yield can be expressed as

$$n_{\rm DT} = 2N\mathcal{B}_{\rm ST}\mathcal{B}_{\rm L}\epsilon_{\rm DT}, \tag{3}$$

where $\mathcal{B}_{\rm L}$ is the leptonic decay branching fraction, including the subbranching fraction of $\tau^+ \to e^+\nu_e\bar{\nu}_\tau$ decay, $\epsilon_{\rm DT}$ is the efficiency of finding the ST and the leptonic decay in the same event. From the ST and DT yields we can obtain an absolute branching fraction of the leptonic decay $\mathcal{B}_{\rm L}$, without needing to know the integrated luminosity or the produced number of $D_s^{*\pm}D_s^{\mp}$ pairs,

$$\mathcal{B}_{\rm L} = \frac{n_{\rm DT}}{n_{\rm ST}}\frac{\epsilon_{\rm ST}}{\epsilon_{\rm DT}} = \frac{n_{\rm DT}/\epsilon}{n_{\rm ST}}, \tag{4}$$

where $\epsilon(\equiv \epsilon_{\rm DT}/\epsilon_{\rm ST})$ is the effective signal efficiency. Because of the large solid angle acceptance with high segmentation of the CLEO-c detector and the low multiplicity of the events with which we are concerned, $\epsilon_{\rm DT} \approx \epsilon_{\rm ST}\epsilon_{\rm L}$, where $\epsilon_{\rm L}$ is the leptonic decay efficiency. Hence, the ratio $\epsilon_{\rm DT}/\epsilon_{\rm ST}$ is insensitive to most systematic effects associated with the ST, and the signal branching fraction $\mathcal{B}_{\rm L}$ obtained using this procedure is nearly independent of the efficiency of the tagging mode.

A. Event and tag selection

To minimize systematic uncertainties, we tag using three two-body hadronic decay modes with only charged particles in the final state. The three ST modes[1] are $D_s^- \to \phi\pi^-$, $D_s^- \to K^-K^{*0}$, and $D_s^- \to K_S^0K^-$. Using these tag modes also helps to reduce the tag bias which would be caused by the correlation between the tag side and the signal side reconstruction if tag modes with high multiplicity and large background were used. The effect of the tag bias $b_{\rm tag}$ can be expressed in terms of the signal efficiency ϵ defined by

$$\epsilon = \frac{\epsilon_{\rm DT}}{\epsilon_{\rm ST}} = \frac{\epsilon_{\rm DT}}{\epsilon'_{\rm ST}}\frac{\epsilon'_{\rm ST}}{\epsilon_{\rm ST}} = \frac{\epsilon_{\rm L}\epsilon'_{\rm ST}}{\epsilon'_{\rm ST}}\frac{\epsilon'_{\rm ST}}{\epsilon_{\rm ST}} = \epsilon_{\rm L}b_{\rm tag}, \tag{5}$$

where $\epsilon'_{\rm ST}$ is the ST efficiency when the recoiling system is the signal leptonic decay with single $e^{\pm}$ in the other side of the tag. As the general ST efficiency $\epsilon_{\rm ST}$, when the recoiling system is any possible D_s decays, will be lower than the $\epsilon'_{\rm ST}$, sizable tag bias could be introduced if the multiplicity of the tag mode were high, or the tag mode were to include neutral particles in the final state. As shown in Sec. IV, this effect is negligible in our chosen clean tag modes.

The $K_S^0 \to \pi^+\pi^-$ decay is reconstructed by combining oppositely charged tracks that originate from a common vertex and that have an invariant mass within ± 12 MeV of the nominal mass [3]. We require the resonance decay to satisfy the following mass windows around the nominal masses [3]: $\phi \to K^+K^-$ ($\pm$ 10 MeV) and $K^{*0} \to K^+\pi^-$ ($\pm$ 75 MeV). We require the momenta of charged particles to be 100 MeV or greater to suppress the slow pion background from $D^*\bar{D}^*$ decays (through $D^* \to \pi D$). We identify an ST by using the invariant mass of the tag $M(D_s)$ and recoil mass against the tag $M_{\rm recoil}(D_s)$. The recoil mass is defined as

$$M_{\rm recoil}(D_s) \equiv \sqrt{(E_{ee} - E_{D_s})^2 - |\mathbf{p}_{ee} - \mathbf{p}_{D_s}|^2}, \tag{6}$$

where $(E_{ee}, \mathbf{p}_{ee})$ is the net four-momentum of the e^+e^- beam, taking the finite beam crossing angle into account; $(E_{D_s}, \mathbf{p}_{D_s})$ is the four-momentum of the tag, with E_{D_s} computed from $\mathbf{p}_{D_s}$ and the nominal mass [3] of the D_s meson. We require the recoil mass to be within 55 MeV of the D_s^* mass [3]. This loose window allows both primary and secondary D_s tags to be selected.

To estimate the backgrounds in our ST and DT yields from the wrong tag combinations (incorrect combinations that, by chance, lie within the $\Delta M(D_s)$ signal region), we use the tag invariant mass sidebands. We define the signal region as -20 MeV $\le \Delta M(D_s) < +20$ MeV, and the sideband regions as -55 MeV $\le \Delta M(D_s) < -35$ MeV or $+35$ MeV $\le \Delta M(D_s) < +55$ MeV, where $\Delta M(D_s) \equiv M(D_s) - m_{D_s}$ is the difference between the tag mass and the nominal mass. We fit the ST $\Delta M(D_s)$ distributions to the sum of double-Gaussian signal function plus second-degree Chebyshev polynomial background function to get the tag mass sideband scaling factor. The invariant mass distributions of tag candidates for each tag mode are shown in Fig. 1 and the ST yield and $\Delta M(D_s)$ sideband scaling factor are summarized in Table I. We find $n_{\rm ST} = 26\,334 \pm 213$ summed over the three tag modes.

B. Signal-event selection

A DT event is required to have a ST, a single e^+, no additional charged particles, and the net charge of the event $Q_{\rm net} = 0$. We require the momentum of the e^+ candidate be at least 200 MeV.

[1]The notations $D_s^- \to \phi\pi^-$ and $D_s^- \to K^-K^{*0}$ are shorthand labels for $D_s^- \to K^-K^+\pi^-$ events within mass windows (described below) of the ϕ peak in $M(K^+K^-)$ and the K^{*0} peak in $M(K^+\pi^-)$, respectively. No attempt is made to separate these resonance components in the $K^+K^-\pi^+$ Dalitz plot.

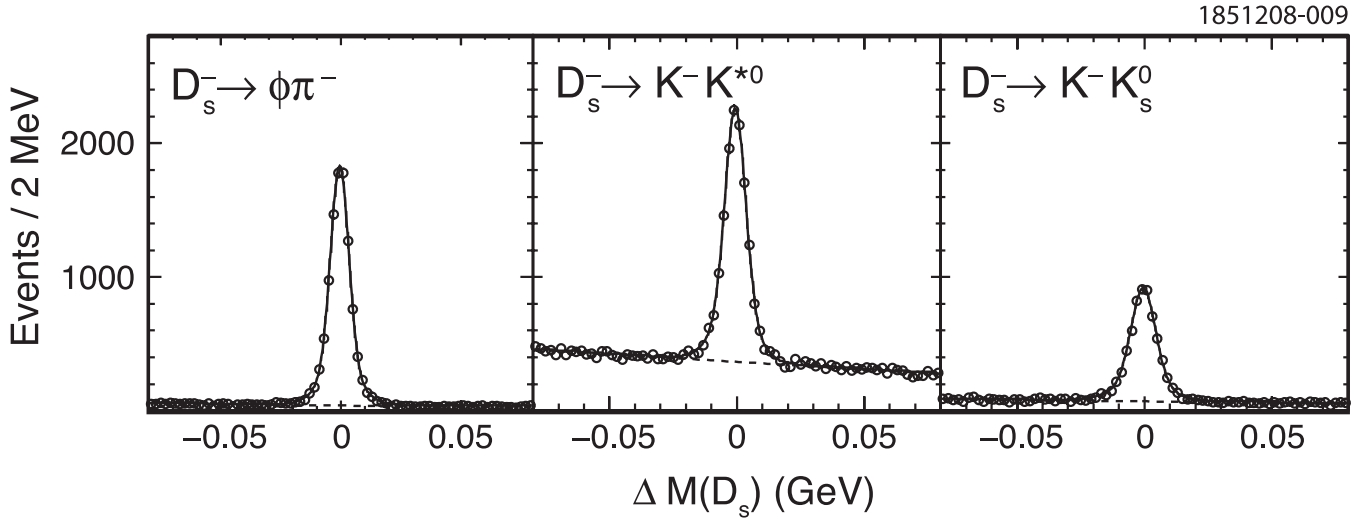

FIG. 1. The mass difference $\Delta M(D_s) \equiv M(D_s) - m_{D_s}$ distributions in each tag mode. We fit the $\Delta M(D_s)$ distribution (open circle) to the sum (solid curve) of signal function (double Gaussian) plus background function (second-degree Chebyshev polynomial, dashed curve).

TABLE I. Summary of single-tag (ST) yields, where $n_{\rm ST}^{\rm S}$ is the yield in the ST mass signal region, $n_{\rm ST}^{\rm B}$ is the yield in the sideband region, s is the sideband scaling factor, and $n_{\rm ST}$ is the scaled sideband-subtracted yield.

Tag mode	$n_{\rm ST}^{\rm S}$	$n_{\rm ST}^{\rm B}$	s	$n_{\rm ST}$
$D_s^- \to \phi\pi^-$	10 459	807	0.980	9668.1 ± 106.1
$D_s^- \to K^- K^{*0}$	18 319	7381	1.000	10 938.0 ± 160.3
$D_s^- \to K^- K_S^0$	7135	1409	0.999	5727.8 ± 92.4
Total				26 333.9 ± 213.3

The DT events will contain the sought-after $D_s^+ \to \tau^+ \nu_\tau$ ($\tau^+ \to e^+ \nu_e \bar{\nu}_\tau$) events, but also some backgrounds. The most effective variable for separating signal from background events is the extra energy ($E_{\rm extra}$) in the event, i.e., the total energy of the rest of the event measured in the electromagnetic calorimeter. This quantity is computed using the neutral shower energy in the calorimeter, counting all neutral clusters consistent with being photons above 30 MeV; these showers must not be associated with any of the ST decay tracks or the signal e^+. We obtain $E_{\rm extra}$ in the signal and sideband regions of $\Delta M(D_s)$. The sideband-subtracted $E_{\rm extra}$ distribution is used to obtain the DT yield.

The $E_{\rm extra}$ distribution obtained from data is compared to the MC expectation in Fig. 2. We have used the invariant mass sidebands, defined in Sec. III A, to subtract the combinatorial background. We expect that there will be a large peak between 100 MeV and 200 MeV from $D_s^* \to \gamma D_s$ decays (and from $D_s^* \to \pi^0 D_s$, with a 5.8% branching fraction [3]). Also, there will be some events at lower energy when the photon from D_s^* decay escapes detection. Based on considerations described in the next paragraph, we define our signal region to be $E_{\rm extra} < 400$ MeV.

C. Background estimation

After the $\Delta M(D_s)$ sideband subtraction, two significant components of background remain. One is from $D_s^+ \to K_L^0 e^+ \nu_e$ decay. If the K_L^0 deposits little or no energy in the calorimeter, this decay mode has an $E_{\rm extra}$ distribution very similar to the signal, peaking well below 400 MeV. The second source, other D_s semielectronic decays, rises

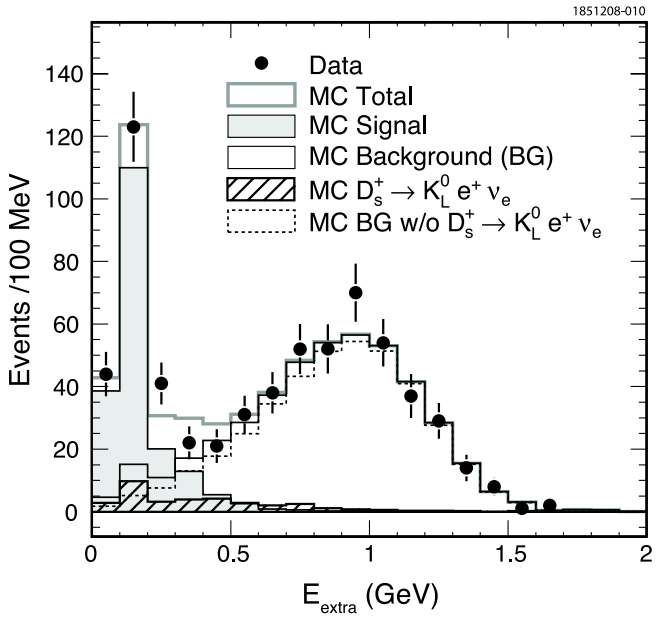

FIG. 2 (color online). Distribution of $E_{\rm extra}$ after $\Delta M(D_s)$ sideband subtraction. Filled circles are from data and histograms are obtained from MC simulation. The MC signal and peaking background ($D_s^+ \to K_L^0 e^+ \nu_e$) components are normalized to our measured branching fractions. The errors shown are statistical only.

TABLE II. Estimated backgrounds in the extra energy signal region below 400 MeV in each tag mode. Here $b_{\rm p}$ is the peaking background from $D_s^+ \to K_L^0 e^+ \nu_e$ decay, $b_{\rm np}$ is the nonpeaking background from other D_s semileptonic decays, and b is the total number of background events. The errors shown are statistical only.

Tag mode	$b_{\rm np}$	$b_{\rm p}$	b
$D_s^- \to \phi\pi^-$	11.8 ± 1.0	7.7 ± 0.5	19.4 ± 1.1
$D_s^- \to K^- K^{*0}$	12.2 ± 1.1	8.7 ± 0.5	20.9 ± 1.3
$D_s^- \to K^- K_S^0$	4.6 ± 0.7	4.5 ± 0.3	9.1 ± 0.7
Total	28.5 ± 1.7	20.9 ± 0.8	49.4 ± 1.8

smoothly with increasing $E_{\rm extra}$, up to 1 GeV. Estimates of these backgrounds are also shown in Fig. 2. The optimal signal region in $E_{\rm extra}$ for DT yield extraction is predicted from a MC simulation study. Choosing $E_{\rm extra}$ less than 400 MeV maximizes the signal significance. Note that with our chosen requirement of $E_{\rm extra} < 400$ MeV, we are including $D_s^+ \to \tau^+ \nu_\tau \gamma$ as signal. However, this is expected to be very small, as the kinetic energy of the τ^+ in the D_s^+ rest frame is only 9.3 MeV and it cannot radiate much.

The number of nonpeaking background events $b_{\rm np}$ in the $E_{\rm extra}$ signal region is estimated from the number of events in the $E_{\rm extra}$ sideband region between 0.6 GeV and 2 GeV, scaled by the MC-determined ratio c_b ($\equiv b^{(\rm l)}/b^{(\rm h)}$) of the number of background events in the $E_{\rm extra}$ signal region, $b^{(\rm l)}$, to the number of events in the $E_{\rm extra}$ sideband region, $b^{(\rm h)}$. The number of peaking background events $b_{\rm p}$ due to the $D_s^+ \to K_L^0 e^+ \nu_e$ decay is determined by using the expected number from MC simulation. The overall expected number of background events in the $E_{\rm extra}$ signal region, b, is computed as follows:

$$b = b_{\rm np} + b_{\rm p} = c_b b^{(\rm h)}({\rm data}) + b(K_L^0 e^+ \nu_e)_{\rm MC}, \quad (7)$$

where $b^{(\rm h)}$(data) is the number of data events in the $E_{\rm extra}$ sideband region and $b(K_L^0 e^+ \nu_e)_{\rm MC}$ is the number of background events due to $D_s^+ \to K_L^0 e^+ \nu_e$ as estimated from our MC simulation. We normalize this quantity using our measured [25] $\mathcal{B}(D_s^+ \to K_S^0 e^+ \nu_e) = (0.19 \pm 0.05 \pm 0.01)\%$. We simulate calorimeter response to K_L^0 using a momentum dependent K_L^0 interaction probability density function obtained from studying $\psi(3770) \to D^0 \bar{D}^0$ events in which the $\bar{D}^0$ has been reconstructed in hadronic tag modes and the D^0 decays to the $K_L^0 \pi^+ \pi^-$ final state.

The numbers of estimated background events from peaking and nonpeaking sources in each tag mode are summarized in Table II.

IV. RESULTS

The signal efficiency determined by MC simulation has been weighted by the ST yields in each mode as shown in Table III. We determine the weighted average signal efficiency $\epsilon = (72.4 \pm 0.3)\%$ for the decay chain $D_s^+ \to \tau^+ \nu_\tau \to e^+ \nu_e \bar{\nu}_\tau \nu_\tau$.

TABLE III. Summary of the signal efficiency determined by MC simulation. Average efficiency ϵ and the tag bias $b_{\rm tag}$ are obtained by using the weighting factor w determined from single-tag yields in data.

Tag mode	w	$\epsilon \equiv \epsilon_{\rm DT}/\epsilon_{\rm ST}$	$b_{\rm tag} = \epsilon'_{\rm ST}/\epsilon_{\rm ST}$
$D_s^- \to \phi\pi^-$	0.3671	0.6964 ± 0.0046	1.0089 ± 0.0058
$D_s^- \to K^- K^{*0}$	0.4154	0.7337 ± 0.0049	1.0061 ± 0.0060
$D_s^- \to K^- K_S^0$	0.2175	0.7536 ± 0.0054	1.0032 ± 0.0065
Average		0.7244 ± 0.0029	1.0065 ± 0.0036

TABLE IV. Summary of double-tag (DT) yields in each tag mode, where $n_{\rm DT}^{\rm S}$ is the DT yield in the tag mass signal region, $n_{\rm DT}^{\rm B}$ is the yield in the tag mass sideband region, s is the tag mass sideband scaling factor, b is the number of estimated background in the extra energy signal region after tag mass sideband scaled background subtraction, and $n_{\rm DT}$ is the background subtracted DT yield. The errors shown are statistical only.

Tag mode	$n_{\rm DT}^{\rm S}$	$n_{\rm DT}^{\rm B}$	s	b	$n_{\rm DT}$
$D_s^- \to \phi\pi^-$	79	1	0.980	19.4 ± 1.1	58.6 ± 9.0
$D_s^- \to K^- K^{*0}$	110	6	1.000	20.9 ± 1.3	83.1 ± 10.8
$D_s^- \to K^- K_S^0$	50	2	0.999	9.1 ± 0.7	38.9 ± 7.2
Total				49.4 ± 1.8	180.6 ± 15.9

The DT yields with the 400 MeV extra energy requirement are summarized in Table IV. We find $n_{\rm DT} = 180.6 \pm 15.9$ summed over all tag modes. Using $\mathcal{B}(\tau^+ \to e^+ \nu_e \bar{\nu}_\tau) = (17.85 \pm 0.05)\%$ [3], we obtain the leptonic decay branching fraction $\mathcal{B}(D_s^+ \to \tau^+ \nu_\tau) = (5.30 \pm 0.47)\%$, where the uncertainty is statistical.

V. SYSTEMATIC UNCERTAINTY

Sources of systematic uncertainties and their effects on the $D_s^+ \to \tau^+ \nu_\tau$ branching fraction determination are summarized in Table V.

We considered six semileptonic decays, $D_s^+ \to \phi e^+ \nu_e$, $\eta e^+ \nu_e$, $\eta' e^+ \nu_e$, $K^0 e^+ \nu_e$, $K^{*0} e^+ \nu_e$, and $f_0 e^+ \nu_e$, as the major sources of background in the $E_{\rm extra}$ signal region. The second dominates the nonpeaking background, and the fourth (with K_L^0) dominates the peaking background. Uncertainty in the signal yield due to nonpeaking background (0.7%) is assessed by varying the semileptonic decay branching fractions by the precision with which they are known [25]. Imperfect knowledge of $\mathcal{B}(D_s^+ \to K^0 e^+ \nu_e)$ gives rise to a systematic uncertainty in our estimate of the amount of peaking background in the signal region, which has an effect on our branching fraction measurement of 3.2%.

TABLE V. Summary of sources of systematic uncertainty and their effects on the branching fraction measurement.

Source	Effect on $\mathcal{B}$ (%)
Background (nonpeaking)	0.7
$D_s^+ \to K_L^0 e^+ \nu_e$ (peaking)	3.2
Extra shower	1.1
Extra track	1.1
$Q_{\rm net} = 0$	1.1
Non electron	0.1
Secondary electron	0.3
Number of tag	0.4
Tag bias	0.2
Tracking	0.3
Electron identification	1.0
FSR	1.0
Total	4.1

We study differences in efficiency, data vs MC events, due to the extra energy requirement, extra track veto, and $Q_{\rm net} = 0$ requirement, by using samples from data and MC events, in which *both* the D_s^- and D_s^+ satisfy our tag requirements, i.e., ''double-tag'' events. We then apply each of the above-mentioned requirements and compare loss in efficiency of data vs MC events. In this way we obtain a correction of 1.6% for the extra energy requirement and systematic uncertainties on each of the three requirements of 1.1% (all equal, by chance).

The non-e^+ background in the signal e^+ candidate sample is negligible (0.4%) due to the low probability ($\sim 0.1\%$ per track) that hadrons (π^+ or K^+) are misidentified as e^+ [26]. Uncertainty in these backgrounds produces a 0.1% uncertainty in the measurement of $\mathcal{B}(D_s^+ \to \tau^+ \nu_\tau)$. The secondary e^+ backgrounds from charge symmetric processes, such as π^0 Dalitz decay ($\pi^0 \to e^+ e^- \gamma$) and γ conversion ($\gamma \to e^+ e^-$), are assessed by measuring the wrong-sign signal electron in events with $Q_{\rm net} = \pm 2$. The uncertainty in the measurement from this source is estimated to be 0.3%.

Other possible sources of systematic uncertainty include $n_{\rm ST}$ (0.4%), tag bias (0.2%), tracking efficiency (0.3%), $e^\pm$ identification efficiency (1%), and FSR (1%). Combining all contributions in quadrature, the total systematic uncertainty in the branching fraction measurement is estimated to be 4.1%.

VI. SUMMARY

In summary, using the sample of 26 334 tagged D_s^+ decays with the CLEO-c detector we obtain the absolute branching fraction of the leptonic decay $D_s^+ \to \tau^+ \nu_\tau$ through $\tau^+ \to e^+ \nu_e \bar{\nu}_\tau$,

$$\mathcal{B}(D_s^+ \to \tau^+ \nu_\tau) = (5.30 \pm 0.47 \pm 0.22)\%, \quad (8)$$

where the first uncertainty is statistical and the second is systematic. This result supersedes our previous measurement [14] of the same branching fraction, which used a subsample of data used in this work.

The decay constant f_{D_s} can be computed using Eq. (1) with known values [3] $G_F = 1.166\,37(1) \times 10^{-5}$ GeV^{-2}, $m_{D_s} = 1968.49(34)$ MeV, $m_\tau = 1776.84(17)$ MeV, and $\tau_{D_s} = 500(7) \times 10^{-15}$ s. We assume $|V_{cs}| = |V_{ud}|$ and use the value 0.974 18(26) given in Ref. [27]. We obtain

$$f_{D_s} = (252.5 \pm 11.1 \pm 5.2)\ \text{MeV}. \quad (9)$$

Combining with our other determination [15] of $f_{D_s} = (263.3 \pm 8.2 \pm 3.9)$ MeV with $D_s^+ \to \mu^+ \nu_\mu$ and $D_s^+ \to \tau^+ \nu_\tau$ ($\tau^+ \to \pi^+ \bar{\nu}_\tau$) decays, we obtain

$$f_{D_s} = (259.5 \pm 6.6 \pm 3.1)\ \text{MeV}. \quad (10)$$

This result is derived from absolute branching fractions only and is the most precise determination of the D_s leptonic decay constant to date.

Our combined result is larger than the recent LQCD calculation $f_{D_s} = (241 \pm 3)$ MeV [9] by 2.3 standard deviations. The difference between data and LQCD for f_{D_s} could be due to physics beyond the SM [11], unlikely statistical fluctuations in the experimental measurements or the LQCD calculation, or systematic uncertainties that are not understood in the LQCD calculation or the experimental measurements.

Combining with our other determination [15] of $\mathcal{B}(D_s^+ \to \tau^+ \nu_\tau) = (6.42 \pm 0.81 \pm 0.18)\%$, via $\tau^+ \to \pi^+ \bar{\nu}_\tau$, we obtain

$$\mathcal{B}(D_s^+ \to \tau^+ \nu_\tau) = (5.62 \pm 0.41 \pm 0.16)\%. \quad (11)$$

Using this with our measurement [15] of $\mathcal{B}(D_s^+ \to \mu^+ \nu_\mu) = (0.565 \pm 0.045 \pm 0.017)\%$, we obtain the branching fraction ratio

$$R = \frac{\mathcal{B}(D_s^+ \to \tau^+ \nu_\tau)}{\mathcal{B}(D_s^+ \to \mu^+ \nu_\mu)} = 10.1 \pm 0.9 \pm 0.3. \quad (12)$$

This is consistent with 9.76, the value predicted by the SM with lepton universality, as given in Eq. (1) with known masses [3].

ACKNOWLEDGMENTS

We gratefully acknowledge the effort of the CESR staff in providing us with excellent luminosity and running conditions. D. Cronin-Hennessy and A. Ryd thank the A. P. Sloan Foundation. This work was supported by the National Science Foundation, the U.S. Department of Energy, the Natural Sciences and Engineering Research Council of Canada, and the U.K. Science and Technology Facilities Council.

[1] N. Cabibbo, Phys. Rev. Lett. **10**, 531 (1963).
[2] M. Kobayashi and T. Maskawa, Prog. Theor. Phys. **49**, 652 (1973).
[3] C. Amsler *et al.* (Particle Data Group), Phys. Lett. B **667**, 1 (2008).
[4] K. Ikado *et al.* (Belle Collaboration), Phys. Rev. Lett. **97**, 251802 (2006).
[5] B. Aubert *et al.* (*BABAR* Collaboration), Phys. Rev. D **77**, 011107 (2008).
[6] A. G. Akeroyd and C. H. Chen, Phys. Rev. D **75**, 075004 (2007); A. G. Akeroyd, Prog. Theor. Phys. **111**, 295 (2004).
[7] J. L. Hewett, arXiv:hep-ph/9505246.
[8] W. S. Hou, Phys. Rev. D **48**, 2342 (1993).
[9] E. Follana, C. T. H. Davies, G. P. Lepage, and J. Shigemitsu (HPQCD Collaboration), Phys. Rev. Lett. **100**, 062002 (2008).
[10] B. I. Eisenstein *et al.* (CLEO Collaboration), Phys. Rev. D **78**, 052003 (2008).
[11] B. A. Dobrescu and A. S. Kronfeld, Phys. Rev. Lett. **100**, 241802 (2008).
[12] D. Cronin-Hennessy *et al.* (CLEO Collaboration), arXiv:0801.3418.
[13] M. Artuso *et al.* (CLEO Collaboration), Phys. Rev. Lett. **99**, 071802 (2007).
[14] K. M. Ecklund *et al.* (CLEO Collaboration), Phys. Rev. Lett. **100**, 161801 (2008).
[15] J. P. Alexander *et al.* (CLEO Collaboration), Cornell University, LEPP Report No. CLNS 08/2044, 2008; preceding Article, Phys. Rev. D **79**, 052001 (2009).
[16] R. A. Briere *et al.* (CESR-c and CLEO-c Taskforces, CLEO-c Collaboration), Cornell University, LEPP Report No. CLNS 01/1742, 2001 (unpublished).
[17] Y. Kubota *et al.* (CLEO Collaboration), Nucl. Instrum. Methods Phys. Res., Sect. A **320**, 66 (1992).
[18] D. Peterson *et al.*, Nucl. Instrum. Methods Phys. Res., Sect. A **478**, 142 (2002).
[19] M. Artuso *et al.*, Nucl. Instrum. Methods Phys. Res., Sect. A **502**, 91 (2003).
[20] R. Brun *et al.*, GEANT 3.21, CERN Program Library Long Writeup Report No. W5013, 1993 (unpublished).
[21] D. J. Lange, Nucl. Instrum. Methods Phys. Res., Sect. A **462**, 152 (2001).
[22] S. Dobbs *et al.* (CLEO Collaboration), Phys. Rev. D **76**, 112001 (2007).
[23] J. P. Alexander *et al.* (CLEO Collaboration), Phys. Rev. Lett. **100**, 161804 (2008).
[24] E. Barberio and Z. Wąs, Comput. Phys. Commun. **79**, 291 (1994).
[25] J. Yelton *et al.* (CLEO Collaboration), arXiv:0903.0601.
[26] N. E. Adam *et al.* (CLEO Collaboration), Phys. Rev. Lett. **97**, 251801 (2006).
[27] I. S. Towner and J. C. Hardy, Phys. Rev. C **77**, 025501 (2008).